ELSEVIER

Journal of Nuclear Materials 258–263 (1998) 1404–1408

journal of nuclear materials

Quantitative visualization of tritium distribution in vanadium by tritium radioluminography

H. Saitoh [a,*], T. Hishi [a], T. Misawa [a], T. Ohnishi [b], Y. Noya [b], T. Matsuzaki [c], T. Watanabe [c]

[a] *Department of Materials Science and Engineering, Muroran Institute of Technology, 27-1 Mizumoto, Muroran 050-8585, Japan*
[b] *Central Institute of Radioisotope Science, Hokkaido University, Kita-ku, Sapporo 060-0815, Japan*
[c] *Department of Mechanical Engineering, Tohoku University, Aramaki, Aoba-ku, Sendai 980-0845, Japan*

Abstract

Tritium luminography which measures the distribution and intensity of β-rays emitted from tritium using an imaging plate (IP) has been applied to pure vanadium to observe the tritium distribution in it quantitatively. It was demonstrated that the tritium distribution at the microscopic area in the specimen was graphically displayed. In one case, the tritium concentration on a grain surface was about three times greater than that on a neighboring grain. The grains with (0 0 1) surface orientation had a tritium activity of 1 Bq/mm^2 while the grains with the grains with (1 1 1) orientation had 0.4 Bq/mm^2 at the present tritium charging condition. The cause of this difference in tritium concentration was due to the morphology of precipitated hydride varying in the surface orientation of the crystalline grain. For the intensity recorded in the IP, the components of the X-rays generated from tritium in the specimen was only 2%.

1. Introduction

Some methods such as tritium autoradiography [1–3] or silver decoration method [4–6] have been utilized to visualize hydrogen distribution in materials. Tritium autoradiography visualizes the tritium distribution in materials as a distribution of silver particles with high sensitivity and high spatial resolution by the photosensitivity of the photographic emulsion to the β-rays. By this method, the distribution of trapped tritium in the lattice defects such as dislocations or precipitates has been successfully observed at the electron microscopic scale. The silver decoration technique is based on the principle that the adsorbed hydrogen reduces the silver ions in the decoration solution into metallic silver. Thus this technique can visualize the distribution of all isotopes of hydrogen, and is effective to observe not the trapped hydrogen but the migrating one. However, these techniques have a difficulty to evaluate the hydrogen concentration at the observed microscopic areas.

Imaging plate (IP) has recently attracted much attention as a new detector for X-rays, β-rays or electron beams [7–11] because it has an extremely high sensitivity and a large recordable range of up to five orders for these radiation rays [12,13]. Thus, not only the observation of tritium distribution like autoradiography but also the determination of the tritium concentration at a microscopic area in metals can be possible using IP. However, the experimental method to observe the radioactive intensity of β-rays in metals using IP, called tritium radioluminography, has not been reported so far to our knowledge.

In the present work, tritium radioluminography was applied to vanadium metal which is a base metal for some candidates of low activation materials in the nuclear fusion reactor. The tritium concentrations at microscopic areas on three surface of the vanadium was examined by means of tritium radioluminography.

2. Experimental

The disk shaped ingot of pure vanadium $t = 10$ mm in thickness was cold rolled into $t = 0.5$ mm to make

* Corresponding author. Tel.: +81 143-47-3203; fax: +81 143-47-3193; e-mail: saitoh@oyna.cc.muroran-it.ac.jp.

0022-3115/98/$19.00
PII: S0022-3115(98)00144-5

plate specimens. The specimens 10 mm × 10 mm × 0.5 mm in size were annealed at 1373 K for 24 h in vacuum and then furnace cooled. These annealed specimens were polished and mirror finished using alumina paste with 0.05 μm particles.

Tritium was added into the specimens by a cathodic charging method at room temperature. The electrolyte, current density and the charging period for one specimen (specimen A) were 0.1 kmol/m^3 NaOH aqueous solution containing tritium of 185 TBq/m^3, 200 A/m^2 and 1 h, respectively, and those for the other specimen (specimen B) were 0.05 kmol/m^3 H_2SO_4 aqueous solution containing tritium of 3.7 PBq/m^3, 500 A/m^2 and 4 h, respectively. After the tritium addition, the specimens were immersed in dilute aqueous solutions of acetic acid, washed with water, rinsed in ethyl alcohol and then dried. The alkaline electrolyte adsorbed on the specimen surface is eliminated by this treatment.

The specimen was put on an IP, Fujix TR2040, which is specially fabricated for low energy β-rays emitters such as tritium. During the exposure, the IP contacted with the specimen and was maintained in a radiation shielding box to prevent undesirable effects by natural radiation. After the exposure, the radioactive intensity of β-rays recorded on the IP was measured by means of an IP reader as a set of digital data of photo-stimulated luminescence (PSL) intensity at the pixel size of 100 μm × 100 μm. After the observation of tritium distribution, the specimen A was electrochemically etched and then its microstructure was observed by means of a scanning electron microscope (SEM). The electron channeling patterns (ECPs) were observed to determine crystal orientations of the surfaces of some grains appearing on the surface of the specimen. For the quantitative analysis of tritium distribution, both the specimen and the tritium microscale (Amersham RPA 510) which contain eight levels of known amounts of tritium were placed on one IP and exposed to it, simultaneously.

The influence of the X-rays generated by the β-rays in vanadium on the recorded intensity in the IP was evaluated using specimen B to measure the intensity of X-rays by means of a Si(Li) solid-state photon detector.

3. Results and discussion

3.1. Visualization of tritium distribution

Fig. 1(a) shows a tritium radioluminograph of pure vanadium specimen (specimen A) exposed for 18 h to the IP after tritium charging, the bright and dark contrasts being observed. This means that the tritium distribution in vanadium is not uniform, and that the IP can be available to observe tritium distribution in vanadium. The bright regions such as ① – ③ in the radioluminograph are the lower radioactive regions, and dark regions such as ④ – ⑥ are the higher radioactive regions. We could obtain the PSL intensity, which is proportional to the radioactive intensity of tritium, in the form line profile and unit area. Fig. 1(b) shows the line profile of the PSL intensity on the line A–B in Fig. 1(a). The intensity varies about three times depending on the positions inside the line.

Fig. 1(c) is a SEM micrograph of specimen A electrochemically etched after the luminograph observation, and Fig. 1(d) is the enlarged picture of the square rounded portion in Fig. 1(c). The contrast in the luminograph in Fig. 1(a) is well correlated to the microstructure of the specimen indicating that the distribution of radioactivity of tritium on the specimen surface bounds that of some grains. In the present tritium charging condition, vanadium hydride with needle-like bright contrast is formed as shown in Fig. 1(d). There were two types of morphologies of vanadium hydride depending on the grains in the specimen, that is, one is with high density of fine hydride and the other is with low density of coarse hydride. We could clearly find that the higher and lower radioactive grains had high density of fine vanadium hydride and low density of coarse hydride, respectively. Thus, we conclude that the differences in tritium concentrations on the specimen surface is attributed to the difference in the density of precipitated vanadium hydride depending on the grains in the specimen.

Fig. 2 ① – ⑥ show ECPs taken from the respective numbered area of ① – ⑥ in Fig. 1(a). The bright regions of ① – ③ have nearly (1 1 1) plane, while the dark regions of ④ – ⑥ have (0 0 1) plane, i.e., (1 1 1) and (0 0 1) oriented grains are the lower and higher radioactive regions, respectively. This difference is caused by the difference in the density of the precipitated hydride. The density of the hydride is high for higher radioactive (0 0 1) oriented grains, and is low for lower radioactive (1 1 1) oriented grains. The behavior of hydrogen permeation through the surface to the interior may depend on the surface orientation.

3.2. Quantitative analysis of tritium distribution

Nextly, we performed an evaluation of the tritium concentration on the specimen surface. For this purpose, we used tritium labeled microscale as the activity standard which contains eight levels of known amounts of tritium activity. Fig. 3(a) shows a tritium radioluminograph of the tritium labeled microscale exposed for 24 h. The relationship between the tritium activity in the microscale and observed PSL intensity is shown in Fig. 3(b), indicating a linear relationship in them. Thus, the surface radioactive intensity of tritium in the

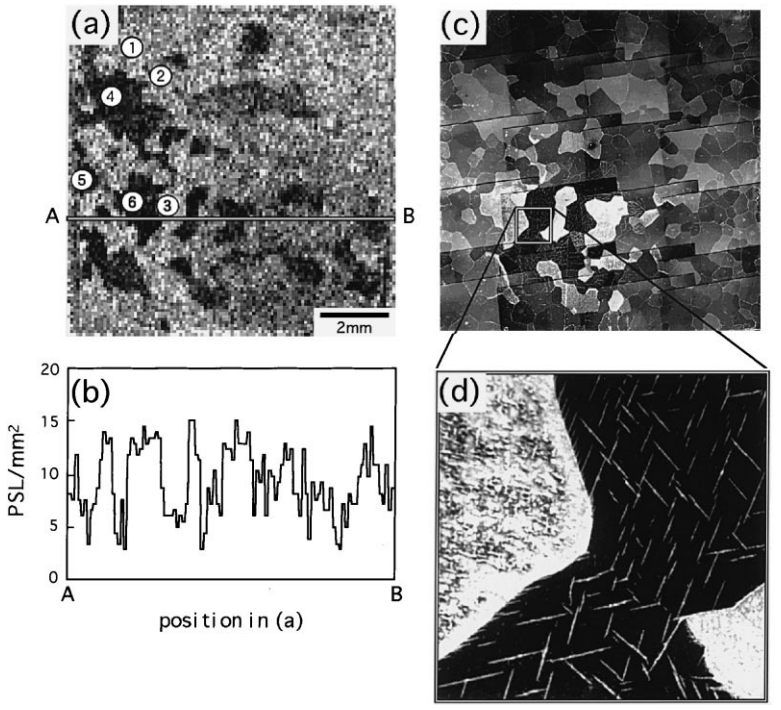

Fig. 1. Tritium radioluminograph of tritium charged pure vanadium (specimen A) exposed for 18 h. Dark and bright regions are the regions with higher and lower radioactivities, respectively. (b) Line profile of the PSL intensity on line A–B in (a). (c) SEM micrograph of the specimens after the radioluminograph observation. The microstructure corresponds well with the contrast of the luminograph. (d) Enlarged picture of (c) showing that the size and density of needle-like vanadium hydride observed in white contrast differs from grain to grain.

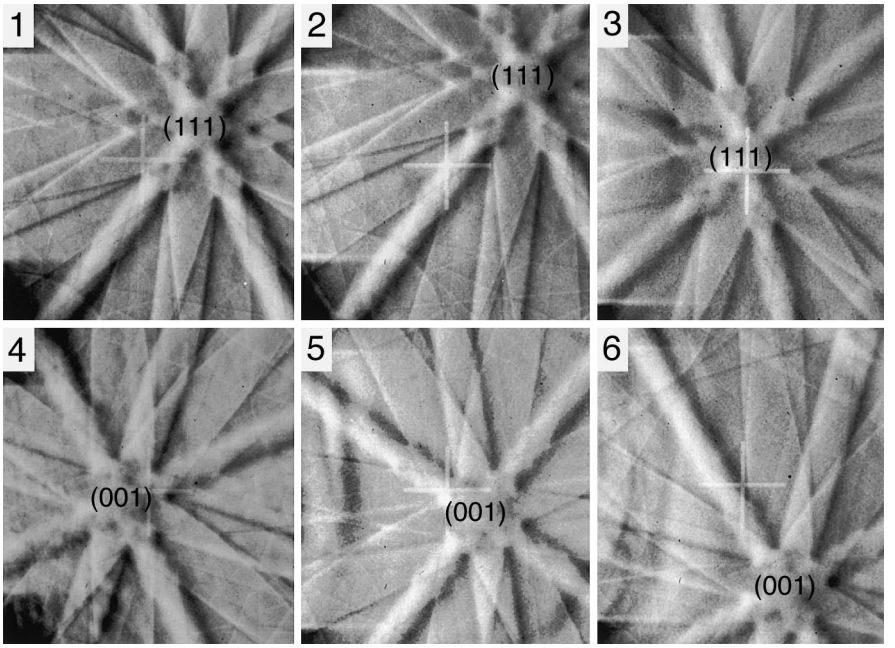

Fig. 2. Electron channeling patterns taken from the respective numbered area of ① – ⑥ in Fig. 1(a) showing that the higher and lower radioactive grains have (0 0 1) and (1 1 1) surface orientations, respectively.

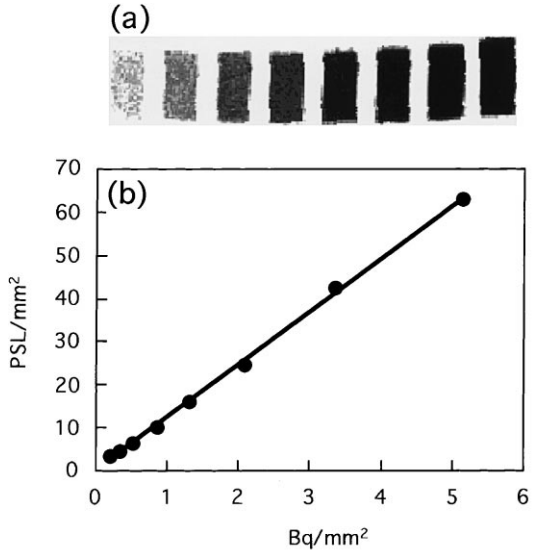

Fig. 3. (a) Tritium radioluminograph of tritium labeled microscale with eight levels of calibrated activity exposed for 24 h. (b) Relation between the tritium activity in the microscale and the PSL intensity observed from the radioluminograph showing a linear relationship.

specimen can be calculated from the observed PSL intensity by using the microscale. If we assume that the mean range of β-rays in vanadium is 0.5 μm, we can evaluate the tritium concentration using the measured surface radioactivity. Table 1 shows the measured PSL value and the calculated concentration of tritium at the region of numbered areas ①–⑥ in Fig. 1(a). It was found that the sensitivity of IP for the tritium was extremely high as can be obtained by ppb order of concentration.

3.3. Effect of characteristic X-ray on radioluminography

The β-rays emitted from tritium dissolved in the vanadium generate continuous bremsstrahlung and characteristic X-rays [14,15]. We also obtained the X-ray spectrum from specimen B using a Si(Li) detector at a present time of 24 h, and confirmed generation of the characteristic X-rays of V-K_α and V-K_β, and bremsstrahlung X-rays. Thus, we examined the effect of X-rays to the PSL value recorded in the IP because the X-rays may affect quantitative analysis by tritium radioluminography.

The measured PSL intensity I_{total} recorded in the IP consists of two components, that is,

$$I_{\text{total}} = I_{\beta\text{-rays}} + I_{\text{X-rays}},$$

where $I_{\beta\text{-rays}}$ and $I_{\text{X-rays}}$ are the intensities of the β-rays and X-rays, respectively. In the present work, $I_{\text{X-ray}}$ was measured using the Saran Wrap (vinylidene chloride film) which was inserted between the specimen and the IP to prevent the irradiation to the IP with β-rays. The obtained I_{total} and $I_{\text{X-rays}}$ of specimen B at the exposure time of 24 h were 2524.0 and 48.3 PSL/mm^2, respectively. Thus the contribution of the X-rays to the radioactive intensity recorded in the IP is about 2%. It is found that most of the intensity recorded in the IP is attributed to the β-rays.

Finally, we compare the sensitivity for X-ray detection by the IP and the Si(Li) detector. The integral counts $I_{\text{Si(Li)}}$ of the X-rays of specimen B between 3 and 6 keV was 7.0×10^4 counts, which corresponds to 2.5×10^3 counts/mm^2. Since $I_{\text{X-rays}}$ of specimen B measured by the IP is 48.3 PSL/mm^2, the ratio $I_{\text{X-rays}}/I_{\text{Si(Li)}}$ is obtained to be 1.9×10^{-2} PSL/counts. Thus, it can be said that for X-ray detection, the IP is less sensitive than the Si(Li) detector.

4. Conclusions

(1) We performed tritium radioluminography to observe the tritium distribution at the microscopic area on vanadium surface. This method was shown to be available to visualize the two dimensional distribution of tritium and to quantify it as higher sensitivity of ppb order.

(2) Tritium concentration in the specimen was about three times different from grain to grain. The grains with (0 0 1) surface orientation have a higher concentration such as 1 Bq/mm^2, and the grains with (1 1 1) orientation have a lower concentration such as 0.4 Bq/mm^2.

(3) Most of the PSL intensity recorded in the IP was due to the β-rays from tritium; the component of the intensity of the X-ray which was generated by the tritium in the specimen was only 2%.

Table 1
Results of the radioactivity and tritium concentration in the respective numbered area in Fig. 1(a) calculated from the measured PSL intensity

Position in Fig. 1(a)	①	②	③	④	⑤	⑥
Intensity (PSL/mm^2)	5.2	4.8	5.0	11.4	12.7	12.7
Radioactivity (10^{-1} Bq/mm^2)	4.2	3.9	4.1	9.3	10.4	10.4
[T] Concentration (at.ppb)	6.6	6.1	6.3	14.4	16.1	16.1

Acknowledgements

This work was supported by Toray Science and Technology Grants from Toray Science Foundation.

References

[1] H. Saitoh, Y. Iijima, K. Hirano, Philos. Mag. B 64 (1991) 113.
[2] H. Saitoh, Y. Iijima, K. Hirano, J. Mater. Sci. 29 (1994) 5739.
[3] H. Saitoh, T. Ohnishi, J. Mater. Sci. Lett. 14 (1995) 417.
[4] T. Schober, C. Dieker, Met. Trans A 14A (1983) 2440.
[5] J. Yao, J.R. Cahoon, Met. Trans. A 21A (1990) 603.
[6] H. Saitoh, T. Hishi, T. Misawa, Mater. Trans. JIM 37 (1996) 373.
[7] Y. Amemiya, J. Synchrotron Radiat. 2 (1995) 13.
[8] K. Takahashi, S. Tazaki, J. Miyahara, J. Karasawa, N. Niimura, Nucl. Instr. Meth. A 377 (1996) 119.
[9] M. Takebe, K. Abe, Y. Kondo, Y. Satoh, M. Souda, Jpn. J. Appl. Phys. 34 (1995) 4197.
[10] H. Ayato, N. Mori, J. Miyahara, T. Oikawa, J. Electron. Microsc. 39 (1990) 444.
[11] M. Sonoda, M. Takano, J. Miyahara, H. Kato, Radiology 148 (1983) 833.
[12] J. Miyahara, K. Takahashi, Y. Amemiya, N. Kamiya, Y. Satou, Nucl. Instr. Meth. A 246 (1986) 572.
[13] BAS Technical Information No. 2, Fuji Photo Film Co, Ltd., Bio-Imaging Analyzer Group.
[14] R. Lässer, Z. Phys. Chem. Neue Folge 143 (1985) 23.
[15] R. Lässer, H. Wenzl, Fusion Technology 1982, Proceedings of the 12th Symposium vol. 2, 1983, p. 783.